LA-UR-15-22823
Approved for public release; distribution is unlimited.

Title: Damaging HMX/HTPB formulations: In-situ compression imaging using X-ray micro computed tomography

Author(s): Patterson, Brian M.
Cordes, Nikolaus Lynn
Tappan, Bryce C.
Thompson, Darla Graff
Manner, Virginia Warren

Intended for: Report

Issued: 2015-04-17

Damaging HMX/HTPB formulations: *In-situ* compression imaging using X-ray micro computed tomography

Brian M. Patterson, Nikolaus Cordes, Bryce Tappan, Darla Thompson, Virginia Manner

Introduction. HMX (octahydro-1,3,5,7-tetranitro-1,3,5,7-tetrazocine) is a powerful high explosive that is routinely used in formulations such as PBX 9501. Much remains to be learned about the performance and mechanical properties of HMX formulations such as these, particularly after dynamic damage has occurred.[1,2] We have prepared formulations with HMX using hydroxyl terminated polybutadiene (HTPB) binder in order to form an explosive that is relatively insensitive to mild stimuli, analogous to PBXN-110 (differing only in substitution of dioctyladipate (DOA) for isodecyl pelargonate). We have been able to image these samples under quasi-static compressive loads using micro X-ray computed tomography (micro-CT). The explosive binder system is unique in that its density is much lower than HMX and allows for distinction of the separate components (HMX crystals, binder, and voids) by micro-CT, which gives us a handle on how damage occurs within these materials. Nano-scale tomographic compression of individual crystals of HMX is also shown. We have made small changes to the mechanical stiffness of the binder system in order to determine how rigidity plays a role in damage of the composite explosive.

Results. Initial formulations were comprised of 88% HMX, 5.4% HTPB, 5.4% dioctyladipate (DOA), 0.5% methylene diphenyl isocyanate (isonate), 0.7% lecithin, and trace dibutyltin dilaurate as catalyst. Samples have undergone safety testing at LANL, with measurements of impact (62.2 cm), spark (0.0625 J), and friction (199 N); the material is approved for 500 g batches. Four samples (formulations 1 – 4; Table 1) were provided for micro-CT imaging. Samples 1 and 2 were prepared with identical materials (as small ~5mm diameter cylinders using brass cork borers), although sample 1 was mixed by hand on a 10 g scale and sample 2 was mixed using a high-shear remote mixer on a 500 g scale. To examine how the rigidity affects damage properties and produce more rigid samples (Figure 1), samples 3 and 4 were prepared on 5 g scales with slightly increased amounts of isonate (Table 1).

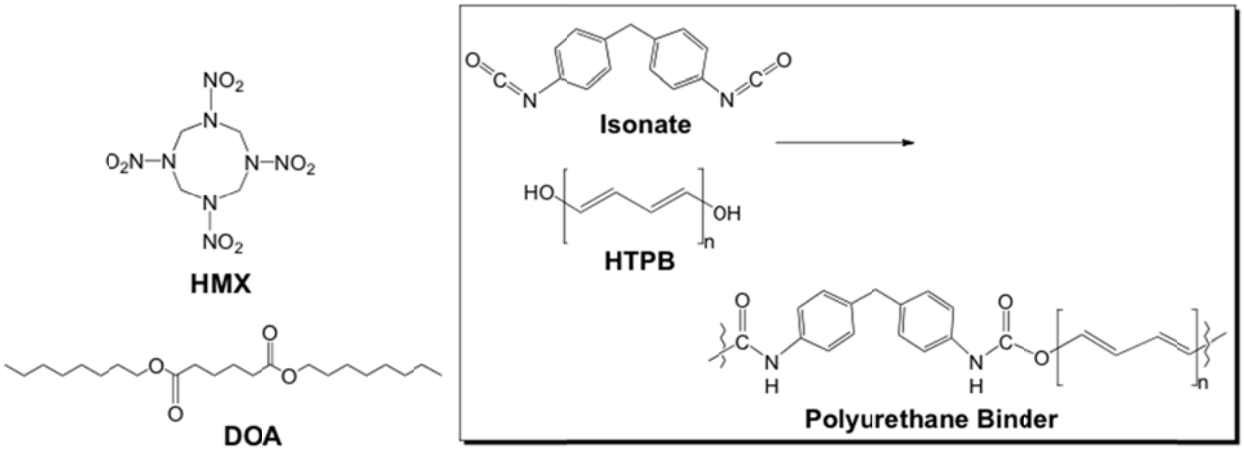

Figure 1. Chemical components of HMX/HTPB formulation, where HTPB crosslinks with Isonate to form the polyurethane binder system surrounding the HMX crystals and DOA performs as a plasticizer.

Table 1. HMX/HTPB formulations prepared and tested

Formulation	% HMX [a]	% HTPB	% DOA	% Isonate	Description
1	88.0	5.40	5.40	0.50	Hand mix, small scale
2	88.0	5.40	5.40	0.50	High shear mixer, large scale
3	87.7	5.38	5.38	0.85	Hand mix, small scale, higher Isonate
4	87.4	5.36	5.36	1.21	Hand mix, small scale, highest Isonate

[a] All HMX is a mixture of 70/30 course/fine.

The samples were each sequentially 3D imaged using an *in-situ* load cell at increasing compressions. Imaging conditions included: 40 kVp, 10W using a W X-ray tube, over 1000 radiographs as the sample was rotated 180^{o} using a Carl Zeiss Microscopy Inc. MXCT system. They were each imaged at two resolutions (11.1 and 2.8 μm voxel sizes), one to encompass the entire sample, the second image to better resolve the crystals. The samples were then uniaxially compressed within a Deben load cell. They were held for 10-15 minutes after compression to allow any residual plastic flow to occur, then imaged at this strain. Each cycle required approximately 26 hours. A single reconstructed slice out of the full 3D data set at several strains for samples 2-4 shown in Figure 2. Samples 1 (not shown) and 2 exhibit a strong visco-plastic flow during uniaxial compression, leading to a large Poisson effect, little cracking or separation of the binder from the crystals. However, samples 3 and 4, were much more rigid and separation between the binder and crystals is widely seen. The separation between the crystals and binder is not uniform throughout the cylinders.

For these materials, excellent X-ray contrast was seen between the HTPB binder, the HMX crystal, and voids, allowing for the segmentation of the material for each. A segmented volume rendering is shown in Figure 3 (left). This segmentation leads to direct measurements of individual crystal and void sizes and locations.

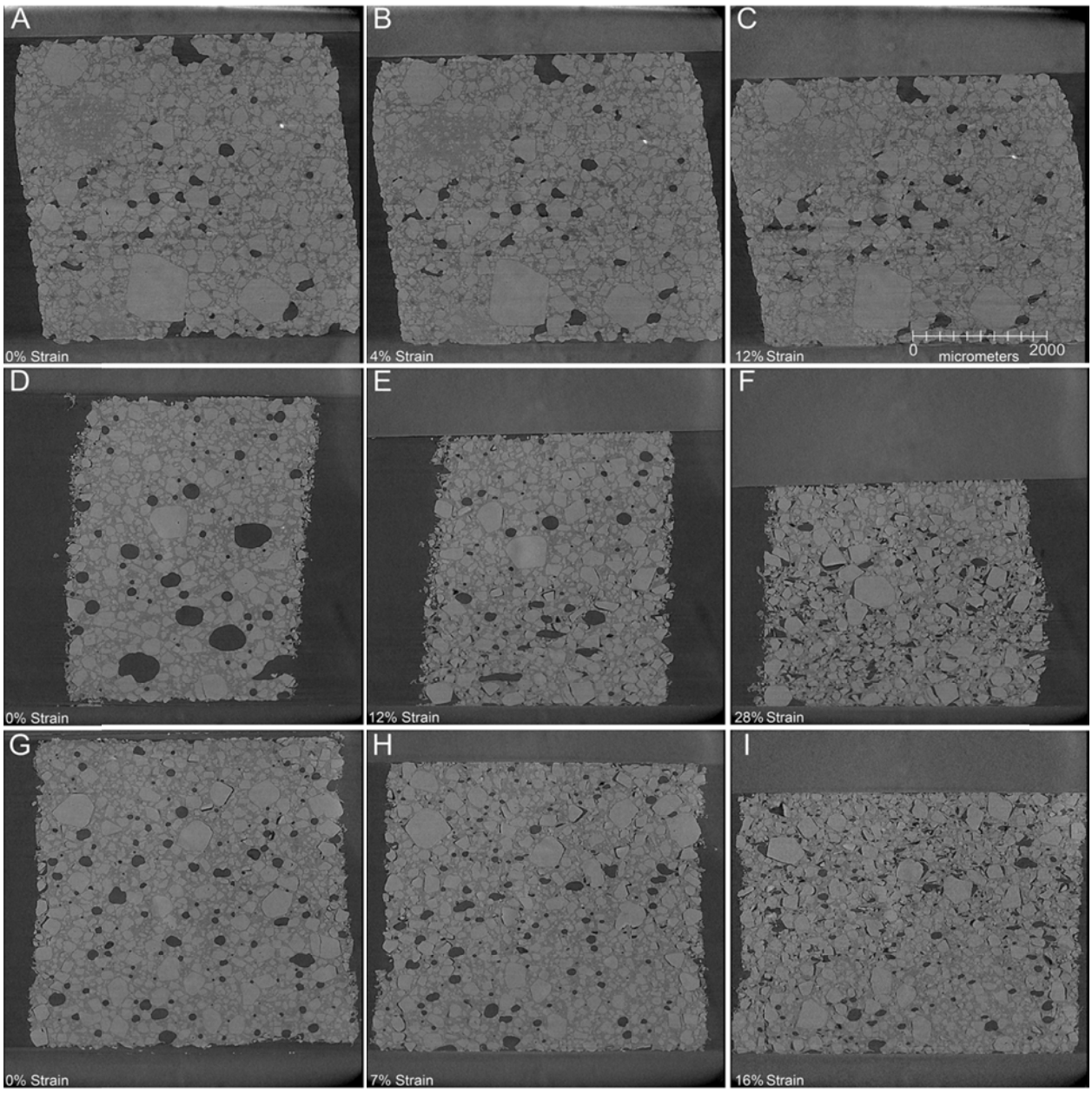

Figure 2. Comparison of samples 2 (A-C), 3 (D-F), and 4 (G-I) uncompressed, (A,D,G) and at different uniaxial strains. Note that sample two does not show cracking, but mostly flow. Samples 3 and 4 show a separation of the binder from the crystals.

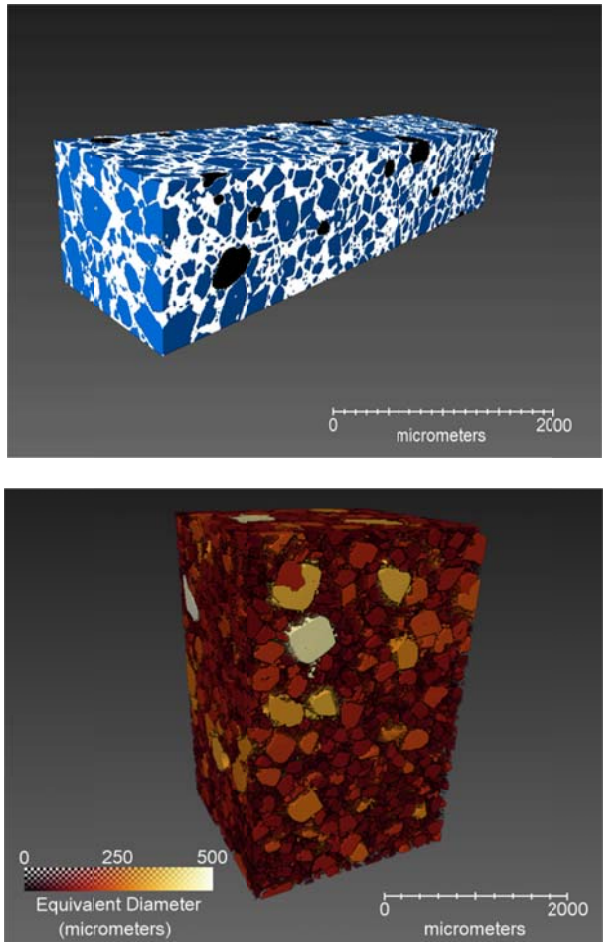

Figure 3. TOP: Volume rendering of Sample 1, showing HMX crystals (blue), HTPB binder (white), and voids within the HMX/HTPB explosive (black). **BOTTOM:** Volume rendering of the HMX crystals in a cropped section of sample 3. HMX crystals are colored by equivalent diameter.

Discussion. Samples 1 – 4 exhibit sufficient contrast within the CT image data sets to allow for segmentation and measurement of individual HE components. This is an important observation, as most X-ray tomography studies of PBX materials have given poor contrast between the crystals and binder to date. With this segmentation, we can label individual crystals and record many morphological measures such as their size, shape, location and their distribution variations.

Table 2 gives the observed percent volume and mass for the HMX crystals, binder, and voids in each of the samples. For samples 1 and 2, identical percent by *volumes* of crystals, binder and voids were measured, indicating that the two methods of production produced identical crystal/binder distribution. Samples 3 and 4 were prepared with higher levels of isonate, (0.85 and 1.21%, respectively) in order to increase rigidity of the sample without changing the structure. Although samples 1 and 2 are very similar, sample 4 has more void volume than the other samples, potentially due to the rigidity of the sample restricting gas flow, increasing void growth. Figure 2 shows that small cracks are apparent in Sample 4 even before compression.

Table 2. HMX/HTPB formulations: volume and mass percent for each sample

Formulation	% HMX Volume	% Binder Volume	% Void Volume	% HMX Mass	% Binder Mass
1	57.5	37.8	4.7	76.5	23.5
2	57.6	37.9	4.5	76.1	23.9
3	52.8	40.0	7.2	73.4	26.6
4	54.2	39.2	6.6	74.3	25.7

Mass calculations assume a crystal and binder density of 1.905 g $cm^{-3}$and 0.910 g cm^{-3} respectively.

The brittleness of sample 4 means that pouring the solid cylinders of material into a petri dish, released individual crystal of HMX. These crystals were placed onto a 500 micrometer diameter platen on a load cell. A 100 micrometer diameter diamond anvil was brought into contact with the crystal. The HMX crystal was imaged within our Carl Zeiss X-ray Microscopy Inc. UltraXRM nano-scale X-ray microscope imaged using Phase contrast imaging. The sample was then slightly compressed, 5 micrometers, 14 milliNewtons of force, and imaged a second time, Figure 4. Cracks are seen in the uncompressed sample that opens further upon compression (left side of image). Also seen are individual stress regions that have begun to separate (right side of image).

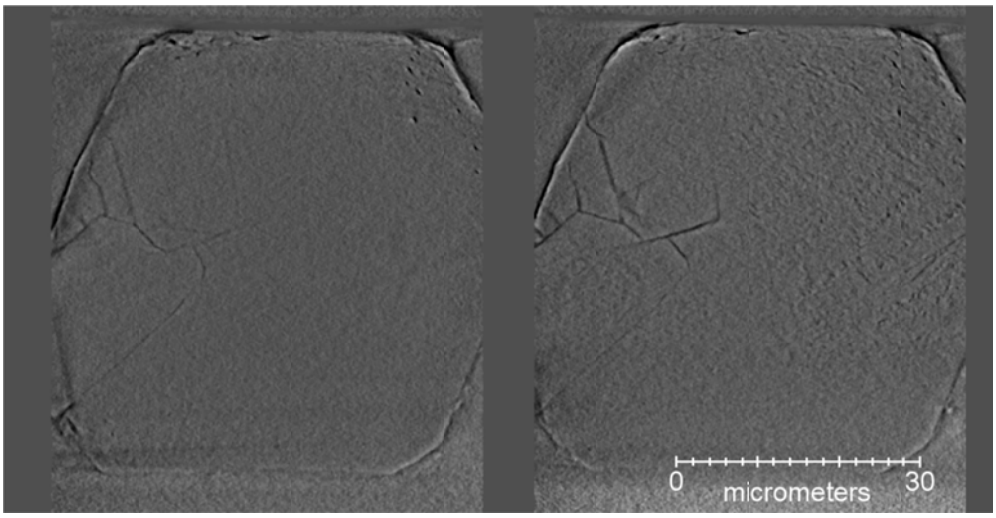

Figure 4. Reconstructed slice through a single HMX crystal from sample 4, uncompressed (left) and compressed by 5 micrometers (right) using phase contrast nano-scale tomography. Crystal is approximately 60 micrometers in diameter, resolution is 150 nanometers.

Future Work:

Taylor Gun: We have used an intermediate-rate gas gun to perform Taylor impact tests on several PBX explosives.[3,4,5] In these experiments, three-inch long PBX projectiles, 0.63 inch in diameter, impact a stationary steel anvil at velocities of 50 to 210 m/s. High-speed cameras are used to capture the side-view and top-view impact distortions in real time, initially with the hope of performing yield stress analysis at these intermediate rates, based on modifications of Taylor's original theory for metals. Our data have shown that even for the softest and most ductile of explosive composites (high performance propellant, HPP, is our example), at ~85 m/s, radial cracks open at the impact tip in the first few frames of images, and material models that cannot accommodate fracture and damage (density change) are not particularly relevant. For this reason, our studies have primarily focused on fragmentation (size distribution) as a

function of impact velocity. The modeling and preliminary imaging studies will be combined with Taylor Gun impact measurements to experimentally determine how these HMX/HTPB samples respond to damage.

For the work proposed here on HMX-based composites very similar to PBXN-110, we are interested to extend our post-impact specimen analysis beyond the quantification of fragment size and number. The demonstrated success of X-ray tomography on identifying crystals, binder and pores promises useful insight to the details of the internal damage caused by dynamic impact.

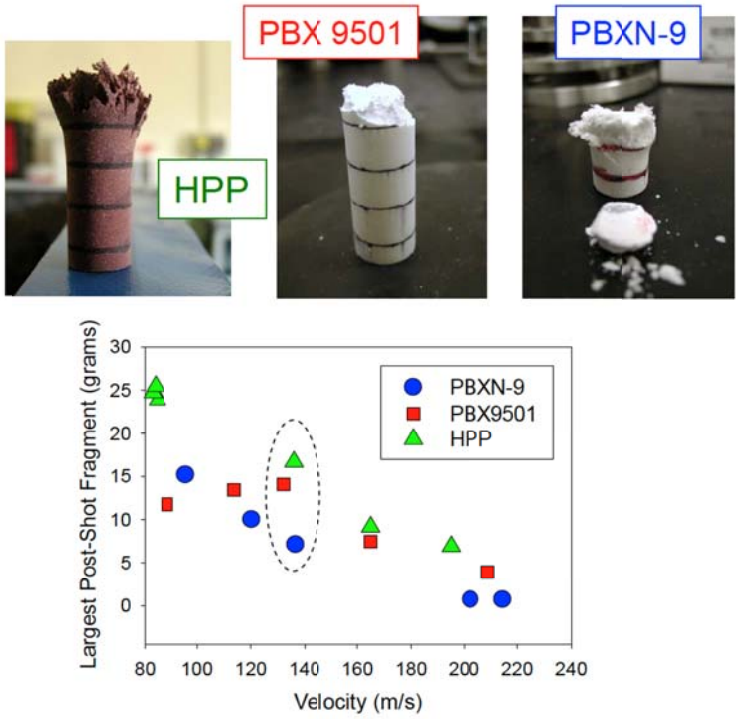

Figure 4. (Bottom) The largest post-shot fragment is plotted versus impact velocity for a number of shots for three different PBX composites; (Top) Photos of the largest post-shot fragment for the tests around 135 m/s (circled in graph) are shown for the three different composites.

In Figure 4 we plot the largest post-shot fragment weight as a function of impact velocity for three different explosives. PBX 9501 and PBXN-9 are both HMX-based, highly–filled and with quite brittle binders, while the binder system of HPP is much softer and more like PBXN-110. For every impact, the back end of the specimen stays intact (see photos), while the front fragments. The size of the rear intact piece is inversely proporational to the velocity,

X-ray tomography of these back end post-impact PBXN-110 composite specimens would allow us to understand the nature of the internal damage that they contain. Tomography would allow us to quantify before- and after-impact changes in pore size and shape distribution, including the potential for anisotropic damage and pore structure. With easily controlled variables such as impact velocity, specimen size, and binder properties (above), we can prepare a wide variety of post-impact specimens for damage characterization and evaluation. For specimens showing unique porosity changes (anisotropy of damage, for example), further performance-based testing may prove interesting. We may also study the

damage of samples under impact, and test the shock sensitivity and run to detonation in damaged samples. Preliminary studies have already been performed with HMX/HTPB mixtures, analyzing the shock to detonation transition via microwave interferometry. Time permitting, this work will be pursued further, and dynamic damage schemes will be investigated. We may also be able to begin a modeling collaboration to investigate how the level of sample rigidity relates to damage in impact experiments.

X-ray Tomography: The work here shows that with micro-CT we measure the crystal size distribution uniformity and lot-to-lot variation in particle and void sizes. The 3D structure can be used as a starting point to mechanical modeling, and tracking individual crystal flow pathways during compression[6]. Analysis of CT data sets at compression points will enable visualization and measurement of HE component (crystal, void) changes due to uniaxial compression. We have demonstrated (with Axinte Ionita) that this data can be entered into COMSOL. Finally, for softer samples that exhibit stress relaxation, information is lost while the stress relaxation occurs. We have demonstrated that it is possible to image polymer foams in which a full 3D image is collected in one second, 20 images within 100 seconds at the synchrotron. It may be possible to do the same with HE, however sample damage may be a problem.

References

1. Arnold, W.; Muthig, H. "What Influences the Shock Sensitivity of High Explosives?" *Insensitive Munitions & Energetic Materials Technology Symposium*, Bristol, UK, April 24 – 28, **2006**.
2. Lee, J.-S.; Hsu, C.-K. "Thermal Properties and Shelf Life of HMX-HTPB Based Plastic-Bonded Explosives," *Thermochimica Acta*, **2002**, 392 – 393, 153 – 156.
3. Ma, X., Zhang, D.Z., Giguere, P.T., Liu, C., "Axisymmetric computation of Taylor cylinder impacts of ductile and brittle materials using original and dual domain material point methods," *Int. J. of Impact Engineering*, 54 (**2013**), 96 – 104.
4. Clements B, Luscher D J, Thompson D G, DeLuca R and Brown G W **2012** Taylor impact tests and simulations of plastic bonded explosives, *AIP Conf. Proc.* **1426** 661.
5. Thompson, D.G., DeLuca, R., Archuleta, J., Brown, G.W., Koby, J., "Taylor Impact Tests on PBX Composites: Imaging and Analysis," *Proceedings of the APS-SCCM*, held in Seattle., WA, July **2013**.
6. Hu, Z.; Luo, H.; Bardenhagen, S. G.; Siviour, C. R.; Armstrong, R. W.; Lu, H. *Exp Mech* **2015**, *55*, 289-300.